

Theory and modelling of optical waveguide sensors utilising surface plasmon resonance

J. Čtyroký^a, J. Homola^a, P. V. Lambeck^b, S. Musa, H. J. W. M. Hoekstra, R. D. Harris^c, J. S. Wilkinson^c, B. Usievich^d, N. M. Lyndin^d

^a Institute of Radio Engineering and Electronics, Academy of Sciences of the Czech Republic, Chaberská 57, 182 51, Prague, The Czech Republic

^b MESA Research Institute, University of Twente, Enschede, The Netherlands

^c Optoelectronics Research Centre, University of Southampton, UK

^d General Physics Institute, Russian Academy of Sciences, Moscow, Russia

1. Introduction

The use of optical waveguides in optical sensors offers numerous advantageous features such as small size, ruggedness, potential for realising various optical functions on a single chip (integration with other optical components), multichannel sensing *etc.* The first integrated optical sensors based on the principle of a surface plasmon resonance (SPR) have been described in late eighties [1, 2]. Since then, integrated optical SPR sensors have been intensively studied and SPR sensing devices using slab waveguides, channel waveguides and even more complex channel waveguide structures have been developed [3, 4, 5, 6, 7]. As the excitation of surface plasmons in guided-wave structures is more complicated than in bulk-optic configurations such as attenuated total reflection method, more sophisticated modelling tools are required for the design and optimisation of SPR integrated-optical sensing structures. For modelling properties of integrated-optical waveguide SPR sensing devices, various methods based on the analysis of properties of waveguide modes have been recently used which differ mainly in the assumed complexity of the interaction among surface plasmon waves (SPW) and waveguide modes.

This is the purpose of this paper to analyse the phenomenon of excitation of SPW's in a simple integrated-optical waveguide structure, and also to compare the performance of existing modelling approaches. We compare here methods developed independently at four laboratories actively working in this field: MESA Research Institute of the University of Twente (UT), the Optical Research Centre of the University of Southampton (ORC), the Institute of Radio Engineering and Electronics of the Academy of Sciences of the Czech Republic, (IRPE), and the General Physics Institute of the Russian Academy of Sciences (GPI). In the first stage, the process of excitation of a SPW in a waveguide structure is described qualitatively, based on the analysis of modal properties of waveguide modes and SPW's. Then, a rigorous approach to analysis of light propagation through a waveguide structure with a metal overlayer supporting SPW's is formulated, as an application of a bi-directional mode expansion propagation method [8]. As the back-reflections in the structure are found to be very weak and most of optical power is transmitted by only a limited number of modes of the sensing structure, the method can be considerably simplified.

2. Surface plasmons

A surface plasmon wave (SPW) is a strongly localised electromagnetic surface wave that propagates along the planar interface between the metallic and dielectric media. Its propagation constant may be expressed as

$$\beta_{SP} = k_0 \sqrt{\frac{\epsilon_d \epsilon_m}{\epsilon_d + \epsilon_m}} \quad (1)$$

where $k_0 = 2\pi/\lambda$ is the angular repetency (the wave number), λ is the free space wavelength, and ϵ_d, ϵ_m are relative permittivities of the dielectric and metal, respectively. The permittivity of metal is generally complex, $\epsilon_m = \epsilon'_m + i\epsilon''_m$. The surface plasmon may exist if the real part of the permittivity of the metal is negative and $\epsilon'_m < -\epsilon_d$. The surface plasmon wave is a TM-polarised (or p-polarised) wave. If the Cartesian co-ordinate system is introduced in which x -axis is perpendicular to the interface and the wave propagates in the z -direction, only the electromagnetic field components E_x, E_z , and H_y are non-zero. The electromagnetic field decreases exponentially with the distance from the interface, with the penetration depths of

$$l_d = \frac{1}{k_0 \epsilon_d} \text{Re}\left\{\sqrt{\epsilon_m + \epsilon_d}\right\}, \quad l_m = \frac{1}{k_0} \text{Re}\left\{\frac{\sqrt{\epsilon_m + \epsilon_d}}{\epsilon_m}\right\} \quad (2)$$

into the dielectric and metal, respectively. It is this strong localisation of energy of the SPW that makes its application for optical sensing attractive.

2.1. Surface plasmon waves supported by a thin metal layer

Solution of the eigenmode equation for a thin metal layer surrounded by two dielectric materials (see insert in Fig. 1) leads to two guided eigenmodes. If the metal layer thickness is large compared to l_m , these eigenmodes are basically the two SPW's localised at the boundaries of the metal layer propagating with the propagation constants given by (1). If the metal layer is rather thin, the two SPW's supported by a single interface become mutually coupled, and therefore the eigenmodes supported by a thin metal layer depart from the isolated SPW's and exhibit more complex properties of their propagation constants and field distributions. If the dielectrics on both sides of the metal layer are identical, the field distribution of these eigenmodes is symmetric and antisymmetric. Unlike the case of modes guided by a dielectric slab waveguide, the propagation constant of the *antisymmetric* SPW eigenmode is *larger* in both real and imaginary part than that of the *symmetric* SPW eigenmode. The antisymmetric mode is sometimes referred as a "short-range" SP, and the symmetric one as a "long-range" SP. In a more general case of different dielectrics at both sides, these properties are essentially preserved, which makes it plausible to use the terms "antisymmetric" and "symmetric" SP in a wider sense even for asymmetric structures.

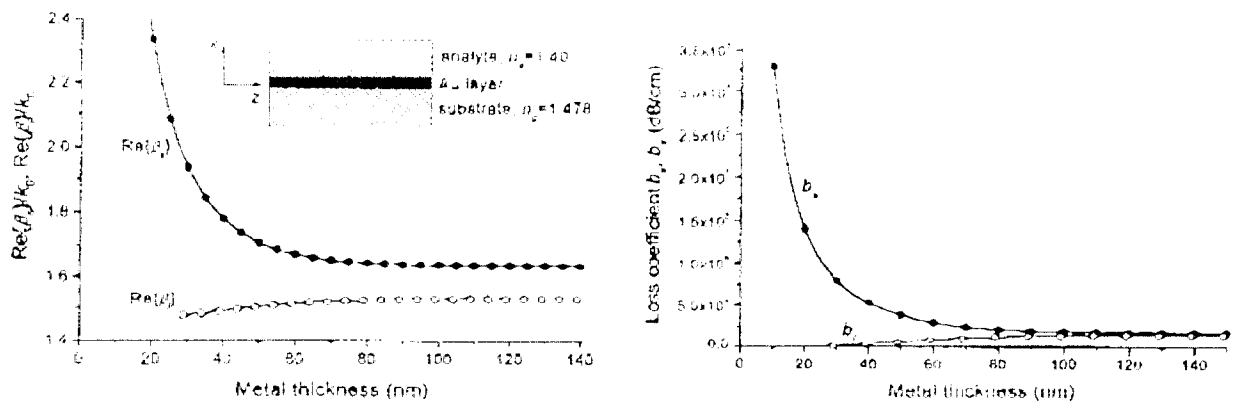


Fig. 1. Propagation and loss constants of SPW's supported by a thin gold layer. β_l and β_s , or b_l and b_s correspond to long-range ("symmetric"), and short-range ("antisymmetric") SPW's, respectively. The wavelength is 633 nm.

The transversal distribution of the module of the transversal component of the magnetic vector $|H_y(x)|$ of both antisymmetric and symmetric plasmons (in this wider sense) supported by a gold film 50 nm thick is illustrated in Fig. 2.

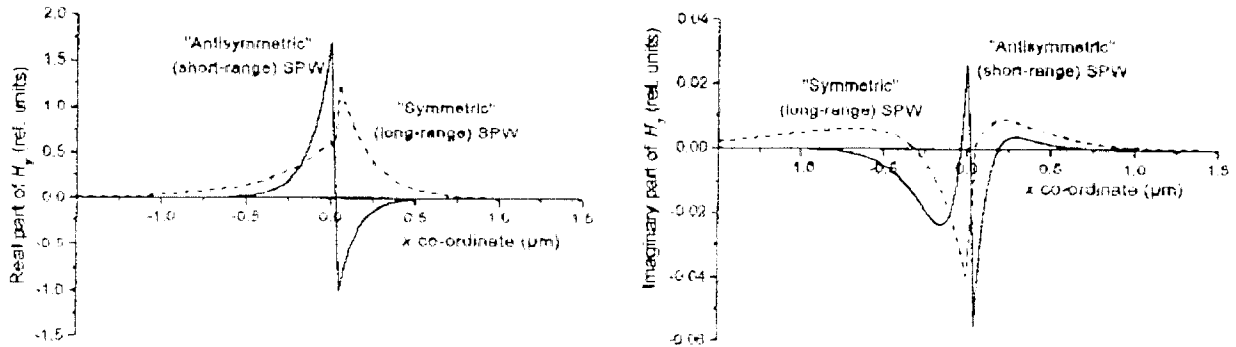


Fig. 2. Magnetic field distribution of short-range and long-range surface plasmons propagating along a gold film 50 nm thick surrounded with dielectrics of refractive indices $n_g = 1.478$ and $n_a = 1.40$. Left – real part, right – imaginary part (note the difference in vertical scales). The wavelength is $\lambda = 633$ nm.

Let us note that when gradually reducing the metal layer thicknesses, the symmetric SPW ceases to exist as a guided wave bound to the metal layer. This critical metal layer thickness is the larger the greater is the asymmetry of the structure. **2.2. Modes supported by a dielectric waveguide with a thin metal overlayer**

As a model waveguiding system we will analyse a simple waveguide configuration (Fig. 3) consisting of a (single-mode) thin-film planar waveguide with a thin metal overlayer.

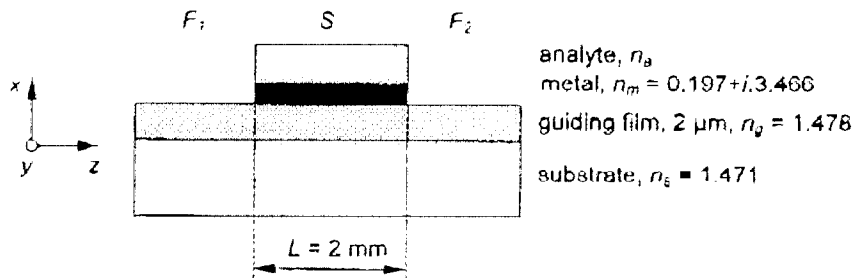


Fig. 3. Basic structure of a waveguide SPR sensor, F are the input and output single-mode film waveguides, S is the sensing section supporting the SPW's.

First the principle of the sensor will be elucidated in a qualitative way, after that the performance will be calculated, applying methods well known from integrated optics for telecommunication components. The light is entering the system from the left as a guided mode of the monomodal section F_1 . Having approached the transition to the sensor section S , the way the light will continue propagating will change, because the field of the incoming mode is no more an eigenmode of the sensor section. What happens is that this incoming mode is decomposed into all guided and radiation modes of the sensing section S , power distribution among these modes being dependent on the field profiles of all modes involved in the decomposition and thus on the physical structure of both sections. At the abrupt waveguide transition, a continuum of radiation modes can be excited, too, but the power transferred to them will be relatively low. Power distribution among the modes as well as their attenuation are strongly dependent on the value of the parameter to be sensed, which is in this case the refractive index of the analyte. Arriving to the next transition $S-F_2$, power of these modes is partially transferred to the guided mode of the output section F_2 . It is this output power of the device that bears the information on the refractive index of the analyte.

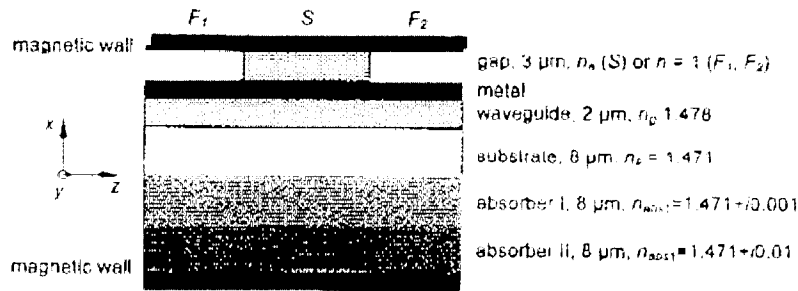


Fig. 4. Modified SPR waveguide structure enclosed between magnetic walls.

The eigenmodes of the sensing section of the waveguide SPR sensor (Fig. 3, section S) can be accurately determined using a transfer matrix approach [9, 10]. A complication can arise when a part of the power of the radiation modes arriving at the second transition should be transferred to the guided mode of the output section, too. This transfer can hardly be accounted for in an exact way. A good and handsome approximation of the real situation can be obtained by enclosing the waveguide structure by two “magnetic walls” that force H_y to be zero there. It is a standard procedure used to discretise the continuous spectrum of modes of open dielectric waveguides [11]. In this way we also exclude leaky modes that are unimportant in our application. In order to suppress the reflections of the waves from the magnetic wall at the substrate side, strongly absorbing layers as shown in Fig. 4 can be used. The reflection from the magnetic wall at the side of an analyte is negligible as the field is very weak there (see Fig. 5.). Strictly speaking, *all* modes of the modified structure in Fig. 4 are guided in the rigorous sense of the word. However, in the following we will use the term “guided modes” only for modes that are guided by the open waveguide structure in Fig. 3, *i.e.*, those localised close to the waveguide layer.

Our calculations will concern the performance of the SPR integrated optical systems with various values of the thickness of the metal layer, namely 30, 40, 50 and 60 nm, and the refractive indices of the analyte n_a varying in the range of 1.3 to 1.45. In this range of parameters, the propagation constants and field distributions of “guided modes” of both waveguide structures in Fig. 3 and Fig. 4 are nearly identical.

The analysis shows that three or two guided TM-polarised modes exist in the waveguide structure, depending on its parameters. The lowest mode (denoted as TM_0) corresponds to the antisymmetric short-range SPW with a very high modal attenuation, and with a considerably higher effective refractive index than the other guided modes. The next two higher order modes represent hybrid modes exhibiting both features of guided mode of a dielectric waveguide and surface plasmon waves. It should be noted that more symmetric structures and those with thicker metal layer support two such hybrid modes while more asymmetric structures and those with thinner metal support only one. More specifically, for the lowest refractive index of an analyte of 1.30, only the next higher mode TM_1 is also guided (*i.e.*, localised near the guiding layer); for higher refractive index of analyte n_a of 1.37 and a thicker gold layer also the third mode TM_2 is guided; for $n_a = 1.40$ the TM_2 mode is guided for both lower and higher gold thicknesses. With increasing n_a the character of the TM_1 mode changes from that similar to the guided mode of the waveguide to that resembling more the symmetric SPW.

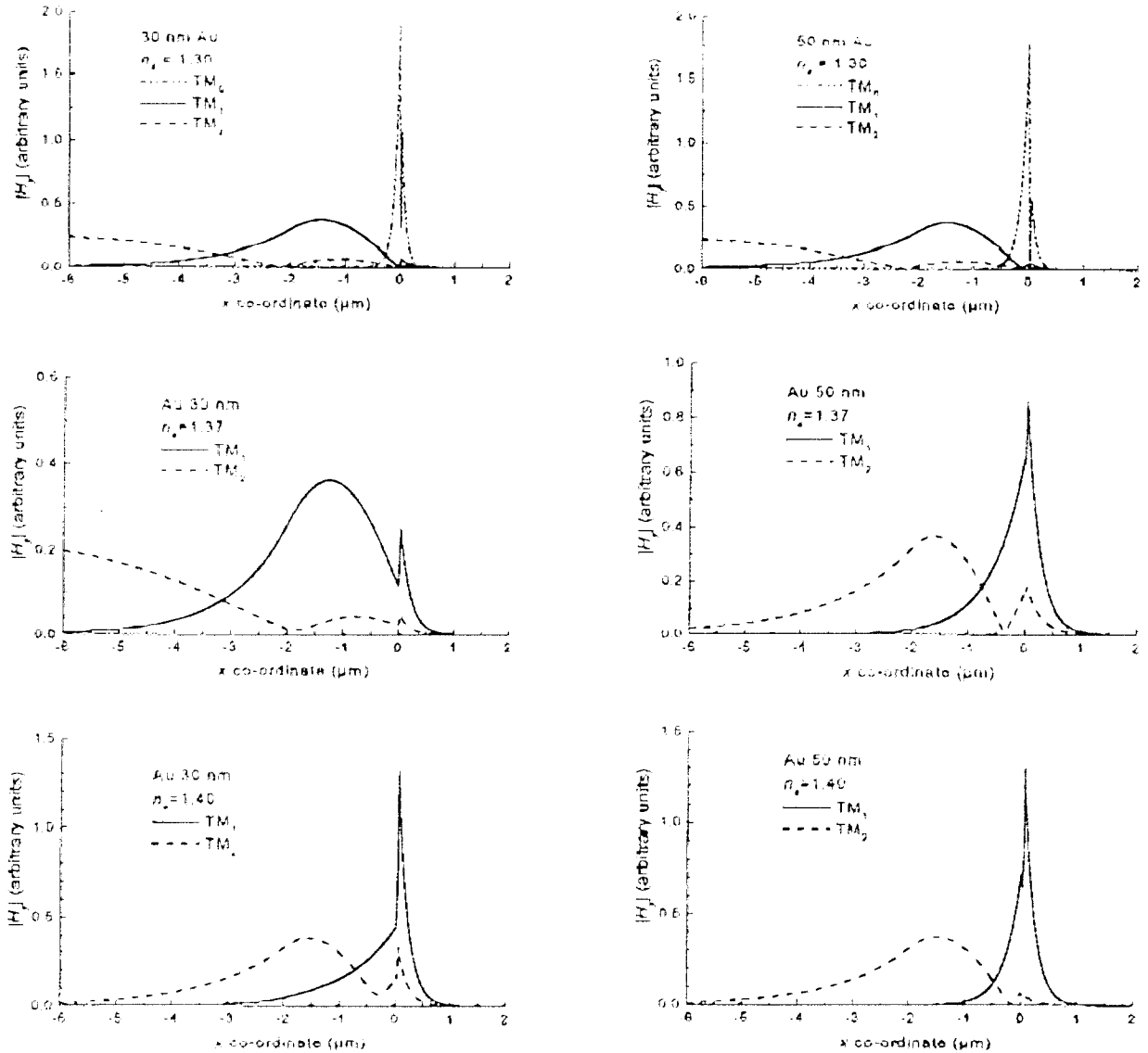


Fig. 5. Field distribution of the lowest-order TM normal modes of the planar waveguide structure supporting SPW's. The parameters are given in the graphs. The TM_0 mode is shown only for $n_a = 1.30$ as its character is only very weakly dependent of n_a .

The dependence of the effective refractive indices and loss coefficients of four lowest-order modes of the sensing section S of the "enclosed" waveguide structure (Fig. 4) on the refractive index of the analyte n_a are plotted in Fig. 6. It is apparent that while the lowest-order mode — the antisymmetric surface plasmon TM_0 — remains unaffected by the presence of the waveguide, it is not the case of the higher-order modes. We observe two different types of behaviour of the guided modes when varying the refractive index of analyte. For rather thin metal layers (see plots for 30nm and 40nm thick gold), as a result of the excitation of SPW, the waveguide modes undergo modal transformation and are reduced to higher order modes when decreasing the refractive index of analyte. In structures with rather thick metal layers the modes maintain their identity and the interaction with SPW is reflected by resonantly enhanced losses of the modes. The refractive index at which the modal transformation or resonant attenuation occur depends on the metal layer thickness, and is the smaller the higher is the metal thickness falling within between 1.39 for 30 nm thick Au layer and 1.36 for 60 nm thick Au layer. This is a consequence of the fact that the propagation constant of the

symmetric SPW increases with increasing the metal layer thickness and decreases with decreasing refractive index of analyte so that these two effects may cancel out each other.

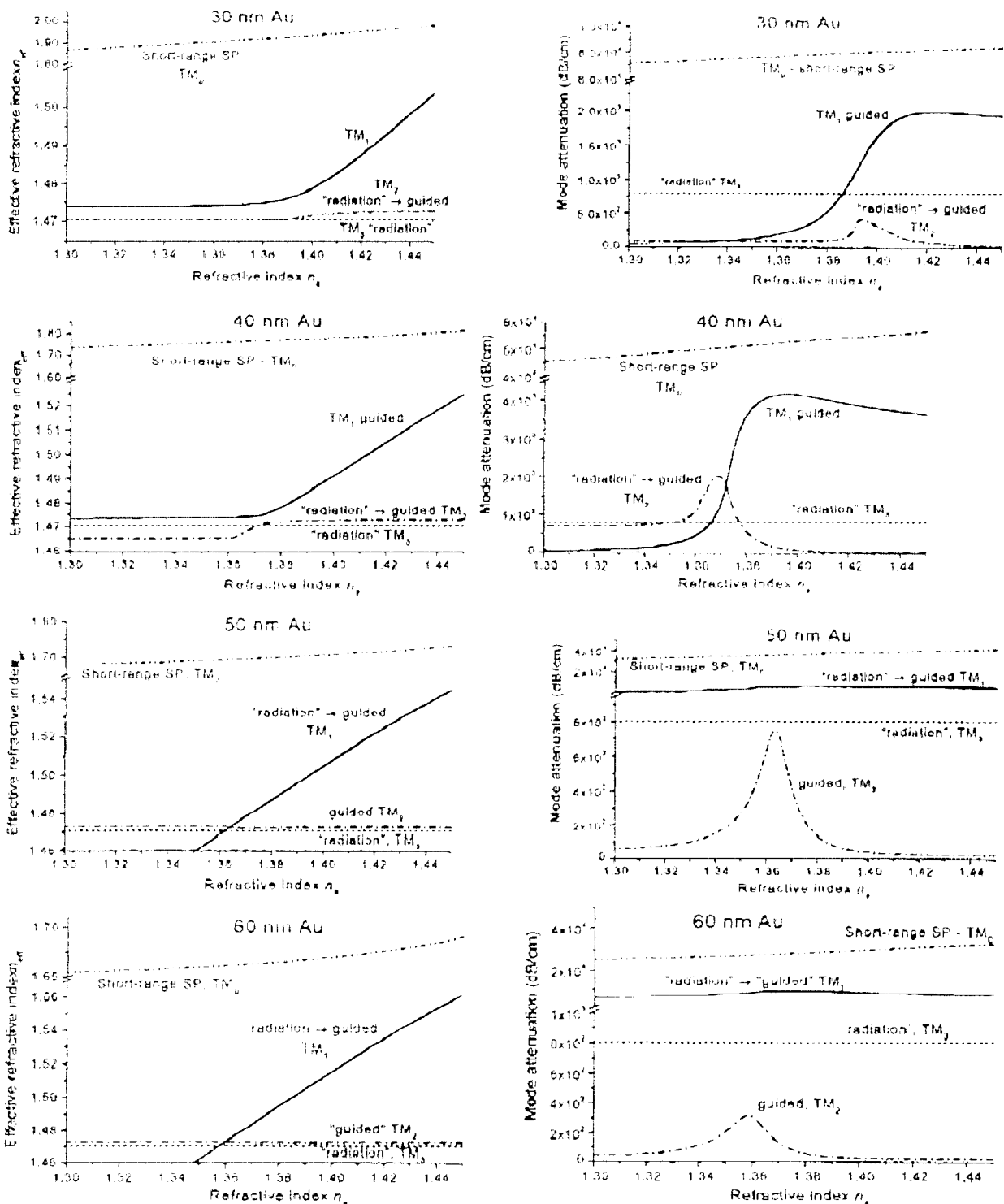


Fig. 6. Modal behaviour of four lowest-order modes of the sensing section S of the waveguide structure in Fig. 4.

3. Modelling transmission through a SPR waveguide sensor

For the design of amplitude waveguide based SPR sensing structures, the dependence of the total optical power transfer from the input waveguide to the output waveguide on the refractive index of analyte needs to be determined. In our modelling we assumed that both the

input and output waveguide sections (denoted as F in Fig. 3 and Fig. 4) are single-mode and the input section is excited by its eigenmode. The task is to calculate the dependence of the output power carried by the mode of the output waveguide on the refractive index of the analyte, n_a , for values of the metal (gold) thickness of 30, 40, 50 and 60 nm. The length of the sensing section is 2 mm, the permittivity of gold is considered to be $\epsilon_m = -11.836107 + 1.357724i$ at the wavelength of 633 nm. The task was solved independently at four research laboratories (UT, ORC, IREE, and GPI). All the groups used, in principle, the same eigenmode expansion and propagation approach in the approximation of which the multiple reflections in the structure are neglected. In order to check the validity of this approximation, IREE used the rigorous BEP method [8,12] to calculate the total back-reflection in the enclosed waveguide structure. It was found that the back reflected power was always below -30 dB, typically in the range of -40 dB to -60 dB, without observable interferences while slightly changing n_a and thus the propagation constants of modes.

Neglecting multiple reflections, the power transfer through the waveguide structure can be expressed by a simple expression

$$p(L) = |a_0(L)/a_0(0)|^2 = \left| \sum_p c_{0p} \exp[i\beta_p L] \right|^2, \quad (3)$$

where $a_0(0)$ and $a_0(L)$ are the complex amplitudes of the fundamental mode of the input and output waveguide (F), respectively,

$$c_{0p} = \frac{\int E_{x,0}^F H_{y,p}^S dx \int E_{x,p}^S H_{y,0}^F dx}{\int E_{x,0}^F H_{y,0}^F dx \int E_{x,p}^S H_{y,p}^S dx} \quad (4)$$

are the coupling coefficients of the fundamental mode of the input and output section F and the p -th mode TM_p of the sensing section S . Here, $E_{x,0}^F, H_{y,0}^F$ and $E_{x,p}^S, H_{y,p}^S$ are the transversal components of the mode fields in the waveguide sections F and S , respectively. If *all* modes of the section S are taken into account, it holds

$$\sum_p c_{0p} = 1. \quad (5)$$

ORC and GPI used this approach for the simulation of the open structure (Fig. 3) with all (*i.e.*, either two or three) localised modes of the sensing section S . In the calculations performed at the UT the contribution of the asymmetrical surfaceplasmon mode to the power transfer has been deliberately neglected because they estimated it to be relatively small. Also they did not calculate attenuations over -60 dB because they were considered to be out of the scope of practical measurements. IREE used 15 lowest order modes of the enclosed waveguide (Fig. 4). It was verified that further increase in the number of modes did not lead to notable changes in the results. The calculated results are plotted in Fig. 7.

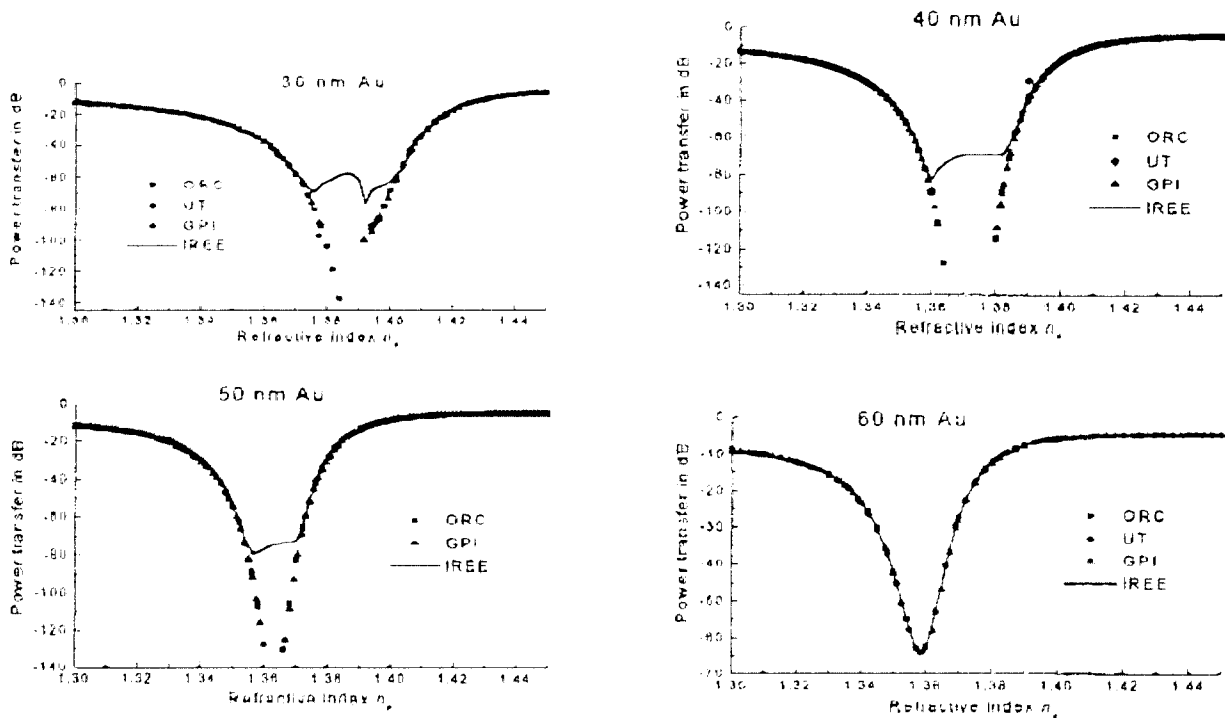


Fig. 7. Dependence of the relative power transfer of the waveguide SPR sensor on the refractive index of the analyte, n_a , as calculated by four laboratories.

4.4 Discussion and conclusions

It may be concluded from Fig. 7 that all the methods give essentially identical results. Apparently the method used by IREE relying on considering a larger number of modes (of an "enclosed" structure) differs from the other methods in the resonant regions where the power transfer of about and less than -60 dB was determined. This difference can be explained by a very small power carried by higher-order modes that are neglected in other methods. It may be objected that residual reflections from the magnetic walls in the "enclosed" structure can increase the power transfer at the resonance significantly. To investigate this, we repeated the calculations for several different positions of the "walls" to allow the reflected waves to combine with different phases. It lead to changes in the order of a few dB in the detailed shapes of the curves only at the power levels below approximately -60 dB. We can thus conclude that the results presented in Fig. 7 are accurate up to this level.

As the results of UT does not differ cognisably from others, it means that the approximation of neglecting the power transfer to the short range SPW (TM_0) is correct. It is the consequence of both its very strong attenuation and very low overlap with the guided mode of the input and output waveguide sections.

We can thus conclude that in systems like this the power transfer to the asymmetrical mode and to radiation modes can be neglected in a very good approximation, and its sensor performance can be calculated by taking into account hybrid modes of the sensor section only. Also some explicit conclusions can be drawn for the performance of the device. In all sensors there are two regions where the dynamic range of the output power is ≈ 50 dB for a refractive index change of about 0.02. Variation of the metal layer thickness causes small shifts of these regions, while also the resolution changes somewhat. Hence the thickness of the metal layer is also one of the parameters suited for tailoring the device to specific applications.

- 1 H.J.M. Kruuwel, P.V. Lambeck, J. van Gent and T.J.A. Popma, "Surface Plasmon Dispersion and Luminiscence Quenching Applied to a Planar Waveguide Sensors for Measurement of Chemical Concentrations", Proc. SPIE vol. 789 (1987) 218–224
- 2 H.J.M. Kruuwel, "Planar Waveguide Sensor for Chemical Domain", PhD Thesis, University of Twente, The Netherlands, 1988
- 3 C.R. Lavers, J.S. Wilkinson, "A Waveguide-Coupled Surface Plasmon Resonance Sensor For An Aqueous Environment", *Sensors and Actuators B*, 22 (1994) 475–81.
- 4 R.D. Harris, J.S. Wilkinson, "Waveguide Surface Plasmon Resonance Sensors, *Sensors and Actuators B*, 29 (1995) 261–267
- 5 M.N. Weiss, R. Srivastava, and H. Grogner, "Experimental Investigation of a Surface Plasmon-Based Integrated-Optic Humidity Sensor," *Electronics Letters* 32 (1996) 842–843
- 6 J. Homola, J. Čtyroký, M. Skalský, J. Hradilová, and P. Kolářova, "A Surface Plasmon Resonance Based Integrated Optical Sensor," *Sensors and Actuators B*, 38–39 (1997) 286–290.
- 7 C. Mouvet, R.D. Harris, C. Maciag, B.J. Luff, J. S. Wilkinson, J. Piehler, Aa. Brecht, G. Gauglitz, R. Abuknesha, and G. Ismail, "Determination of Simazine in Water Samples by Waveguide Surface Plasmon Resonance", *Analytica Chimica Acta*, 338 (1997) 109–117.
- 8 G. Sztafka, and H. P. Nolting, "Bidirectional eigenmode propagation for large refractive index steps," *IEEE Photonics Technology Lett.*, 5 (1993) 554–557.
- 9 J. Chilwell, I. Hodgkinson, "Thin films field-transfer matrix theory of planar multilayer waveguides and reflection from prism-loaded waveguides", *J. Opt. Soc. Am*, A-1 (1984) 742–753.
- 10 T. Itoh, ed., "Numerical Techniques for Microwave and Millimeter Wave Passive Structures". J. Wiley Publishing, New York, 1989.
- 11 R. E. Collin, "Field Theory of Guided Waves", IEEE Press, 2nd ed., (1990).
- 12 J. Čtyroký, J. Homola, M. Skalský, "Modelling of surface plasmon resonance waveguide sensor by complex mode expansion and propagation method", *Optical and Quantum Electronics* 29 (1997) 301–311.